AD-A092 446 BOSTON COLL CHESTNUT HILL MA SPACE DATA ANALYSIS LAB F/G 22/2
ATMOSPHERIC EFFECTS ON THE TIME-VARYING PHOTOELECTRON FLUX FROM--ETC(U)
JUN 80 J M FORBES, H B GARRETT F19628-79-C-0031

UNCLASSIFIED AFGL-TR-80-0185 NL

1 OF 1

AD
A092446

END
DATE
FILMED
1-81
DTIC

LEVEL II

AFGL-TR-80-0185
ENVIRONMENTAL RESEARCH PAPERS, NO. 706

AD A092446

Atmospheric Effects on the Time-Varying Photoelectron Flux From Satellite Surfaces

J. M. FORBES
H. B. GARRETT, Capt, USAF

16 June 1980

SPACE PHYSICS DIVISION PROJECT 7661
AIR FORCE GEOPHYSICS LABORATORY
HANSCOM AFB, MASSACHUSETTS 01731

AIR FORCE SYSTEMS COMMAND, USAF

This report has been reviewed by the ESD Information Office (OI) and is releasable to the National Technical Information Service (NTIS).

This technical report has been reviewed and is approved for publication.

FOR THE COMMANDER

John Howard

Chief Scientist

Qualified requestors may obtain additional copies from the Defense Technical Information Center. All others should apply to the National Technical Information Service.

DISCLAIMER NOTICE

1 AF-L,

viro +1
r rch

Unclassified

SECURITY CLASSIFICATION OF THIS PAGE (When Data Entered)

REPORT DOCUMENTATION PAGE		READ INSTRUCTIONS BEFORE COMPLETING FORM
1. REPORT NUMBER AFGL-TR-80-0185	2. GOVT ACCESSION NO AD-A092446	3. RECIPIENT'S CATALOG NUMBER
4. TITLE (and Subtitle) ATMOSPHERIC EFFECTS ON THE TIME-VARYING PHOTOELECTRON FLUX FROM SATELLITE SURFACES.		5. TYPE OF REPORT & PERIOD COVERED Scientific. Interim.
		6. PERFORMING ORG. REPORT NUMBER ERP No. 706
7. AUTHOR(s) J. M. Forbes* H. B. Garrett, Capt, USAF		8. CONTRACT OR GRANT NUMBER(s) F19 -79
9. PERFORMING ORGANIZATION NAME AND ADDRESS Air Force Geophysics Laboratory (PHG) Hanscom AFB Massachusetts 01731		10. PROGRAM ELEMENT, PROJECT, TASK AREA & WORK UNIT NUMBERS 62101F 76610802
11. CONTROLLING OFFICE NAME AND ADDRESS Air Force Geophysics Laboratory (PHG) Hanscom AFB Massachusetts 01731		12. REPORT DATE 16 June 1980
		13. NUMBER OF PAGES
14. MONITORING AGENCY NAME & ADDRESS (if different from Controlling Office)		15. SECURITY CLASS. (of this report) Unclassified
		15a. DECLASSIFICATION DOWNGRADING SCHEDULE

16. DISTRIBUTION STATEMENT (of this Report)

Approved for public release; distribution unlimited.

17. DISTRIBUTION STATEMENT (of the abstract entered in Block 20, if different from Report)

18. SUPPLEMENTARY NOTES

*Space Data Analysis Laboratory, Boston College, Chestnut Hill, MA 02167

19. KEY WORDS (Continue on reverse side if necessary and identify by block number)

Spacecraft charging
Solar attenuation

20. ABSTRACT (Continue on reverse side if necessary and identify by block number)

Satellites in geosynchronous orbit have been found to vary rapidly in potential as they pass into the earth's shadow. The cause of this effect is known to be the loss of the photoelectron flux from the satellite surface. A material-dependent model of this emission process based on detailed models of the attenuation of the sunlight and of the photoelectron emission as a function of wavelength will be presented. The model is found to agree in detail with actual measurements of photoelectron emission from tungsten. The

DD FORM 1 JAN 73 1473 EDITION OF 1 NOV 65 IS OBSOLETE

Unclassified

SECURITY CLASSIFICATION OF THIS PAGE (When Data Entered)

20. Abstract (Continued)

computer code included in the Appendix is readily adaptable to a number of materials and situations where the detailed absorption of sunlight as a function of altitude is required.

Preface

J. M. Forbes acknowledges support under Air Force Geophysics Laboratory Contract F19628-79-C-0031. Assistance in completing this study was provided by E. G. Mullen. M. Spanos provided typing support. The impetus for the study came from C. Pike.

PRECEDING PAGE BLANK-NOT FILMED

Contents

Illustrations

Illustrations

Atmospheric Effects on the Time-Varying Photoelectron Flux From Satellite Surfaces

1. INTRODUCTION

Although potentials between a satellite and the ambient medium are normally only a few volts (Whipple[1]), potentials as high as -20,000 V during eclipse passage have been observed by geosynchronous satellites (Garrett[2]). In order to analyze the varying potentials during eclipse entry or exit, a detailed understanding of the variation of the solar-generated photoelectron flux is required. As materials can have radically different photoemission properties as a function of wavelength, it is important that the amount of illumination as a function of wavelength be specified. In this paper, a detailed model of photoemission will be derived based on first principles. The model allows a determination of the photoelectron flux as a function of wavelength. Coupled with a model of the atmospheric density, this allows an estimation of the total photoelectron current as a function of satellite position in the earth's penumbra. This latter result permits an accurate determination of the varying satellite potential, given the ambient particle fluxes (Garrett[2]).

The basic theory of time-varying photoelectron flux during eclipse passage was presented in Garrett.[2] Rather than repeat that development, the first section

(Received for publication 10 June 1980)

1. Whipple, E.C. (1965) The Equilibrium Potential of a Body in the Upper Atmosphere, NASA X-615-65-296.

2. Garrett, H.B. (1978) Effects of a Time-V ying Photoelectron Flux on Spacecraft Potential, AFGL-TR-78-0119, A .058 993.

of this paper will start with Eq. (10) of that paper, modified to include the effects of wavelength (an empirical model was assumed for atmospheric attenuation in the original study). This equation is then used to estimate the total attenuated solar flux reaching the satellite. In the second section, the assumed cross sections for the atmospheric constituents will be defined, along with the atmospheric model. The next two sections describe the actual computer programs utilized and compare their output for aluminum and tungsten with experimental results from the INJUN 5 satellite. A listing of the computer programs is included in the Appendix.

2. EQUATIONS AND GEOMETRICAL CONSIDERATIONS

The geometric relationships involved in determining the attenuation of solar flux reaching a satellite due to atmospheric absorption and partial obscuration of the solar disk by the earth have been derived by Garrett.[2] The problem is simplified if the concept of X_m, the minimum ray path altitude, is introduced (see Figure 1). X_m is defined as the minimum distance from the earth that a ray of light attains in going from the center of the sun to the satellite. The problem of finding the percentage of the solar disk that is obscured reduces to that of finding the atmospheric attenuation as a function of X_m rather than of time or position in orbit, which vary greatly for a given satellite.

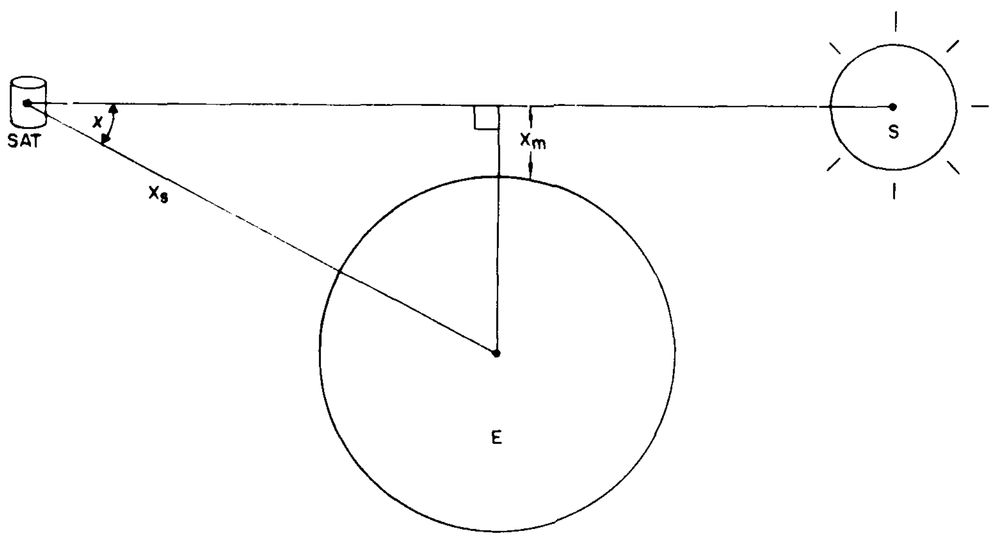

Figure 1. Illustration of the Meaning of χ, the Angle Between the Sun (S) and the Earth's (E) Center, X_s, the Distance from the Satellite (SAT) to the Center of the Earth, and X_m, the Minimum Ray Path Altitude

Referring to Figure 2, and extending Garrett's equations to take into account the dependence on wavelength (λ_m), it can be shown that the value of total flux, F_T, as a function of X_m, is given by:

$$F_T(X_m) = \int_0^{\alpha_{r\odot}} d\theta \int_0^{2\pi} d\phi \int_{\lambda_1}^{\lambda_2} [F(\lambda, X(\theta, \phi))P(\lambda) \sin \theta] d\lambda \qquad (1)$$

where

$X(\theta, \phi)$ = $X_s(\chi') - R_e$ (see Figure 2) = minimum distance of ray to arbitrary point on sun above the earth's surface

χ' = $\cos^{-1} (\cos (\theta) \cos (\chi) + \sin (\theta) \sin (\chi) \cos (\phi))$

$F(\lambda, X)$ = solar flux as a function of λ and X

$\alpha_{r\odot}$ = angular radius of sun (function of day of year)

P = photoemission yield for metal surface

λ = wavelength

θ, ϕ = see Figure 2

X_s = distance from satellite to center of earth.

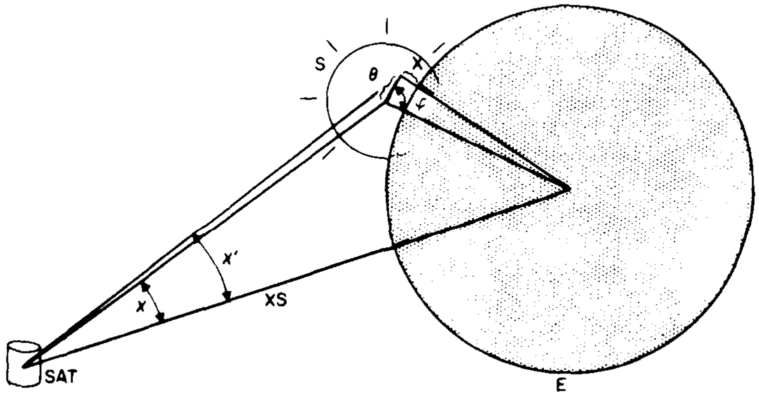

Figure 2. Geometric Representation of the Obscurations of the Solar Disk Upon Eclipse Entry. The variables are defined in the text

The unattenuated photoelectron flux is given by

$$F_T(\infty) = 2\pi(1 - \cos \alpha_{r\odot}) \int_0^{\infty} F(\lambda)P(\lambda)\, d\lambda \tag{2}$$

in electrons-cm^{-2}-sec^{-1} for F_∞ in photons-cm^{-2}-sec^{-1}, or upon dividing by 6.25×10^{18} electron charges/amp-sec, $F_T(\infty)$ is in amp-cm^{-2}. A useful quantity for comparison with observations is the percentage of photoelectron flux, given by

$$P(X_m) = \frac{F_T(X_m)}{F_T(\infty)} \tag{3}$$

The solar flux at λ is obtained by multiplying the unattenuated flux ($F(\lambda)$) by the transmission coefficient ($T(\lambda)$):

$$F(\lambda) = F_\infty(\lambda)T(\lambda) \tag{4}$$

where

$$T(\lambda) = \exp\left[- \sum_{j=1} \sigma_j(\lambda)\, N_j\right] \tag{5}$$

$$N_j = \int_{-a}^{+a} n_j(\xi)\, d\xi \tag{6}$$

n_j = number density of j^{th} species

σ_j = absorption cross section of j^{th} species at wavelength λ (H_2O, O, O_2, O_3, NO, and N_2 were considered)

and ξ is the ray path from the sun to the satellite normal to X_m (see Figure 3). Thus, $\xi = (R_e + Z) \sin \theta$, and it is assumed that zero absorption occurs for $Z > 400$ km.

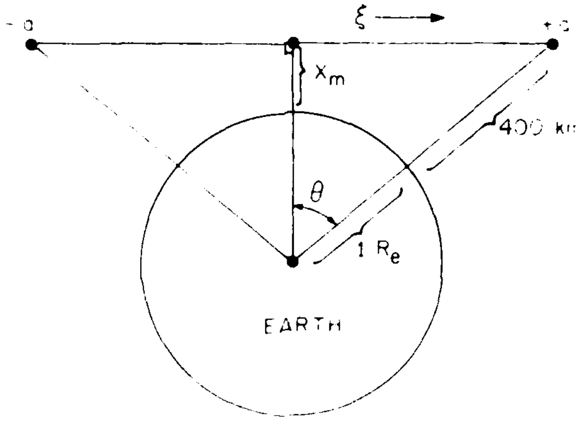

Figure 3. Geometry for Calculation of Column Densities of Absorbing Species

3. INPUT DATA

The unattenuated solar fluxes and O, O_2, O_3, and N_2 cross sections adopted in this study have been obtained from compilations of various experimental data representative of average solar conditions by Strobel[3] for 1260-7500 Å, Richmond[4] for 2-1027 Å, and Keneshea and Huffman[5] for between 1027 and 1260 Å. The NO and H_2O cross sections are from Banks and Kockarts.[6] The solar flux values are shown in Figure 4, and the absorption cross sections are tabulated in the Appendix.

For solar radiation absorption by the O_2 Schumann-Runge bands (1750-2050 Å), we adopt the parameterization used by Strobel[3] for the transmission in each band i, Tr_i:

$$Tr_i = \exp\left\{-\left(\gamma_i I_{O_2} + \delta_i I_{O_2}^{1/2}\right)\right\} \tag{7}$$

---

3. Strobel, D.F. (1976) Parameterization of the Atmospheric Heating Rate from 15 to 120 km Due to O_2 and O_3 Absorption of Solar Radiation, NRL Memorandum Report 3398.
4. Richmond, A.D. (1972) Numerical Model of the Equatorial Electrojet, AFCRL-72-0668, AD 758 196.
5. Keneshea, T.J. and Huffman, R.E. (1972) Solar Photoionization Rate Constants and Ultraviolet Intensities, AFCRL-72-0667, AD 756 480.
6. Banks, P.M. and Kockarts, G. (1973) Aeronomy, Part B, Academic Press, N.Y.

and the cross section of O_2 in each band:

$$\sigma_i = \alpha_i + \beta_i I_{O_2}^{1/2} \tag{8}$$

where I_{O_2} = column density of O_2 along the ray path, and γ_i, δ_i, α_i, and β_i are constants tabulated in subroutine ABSORB (see Appendix).

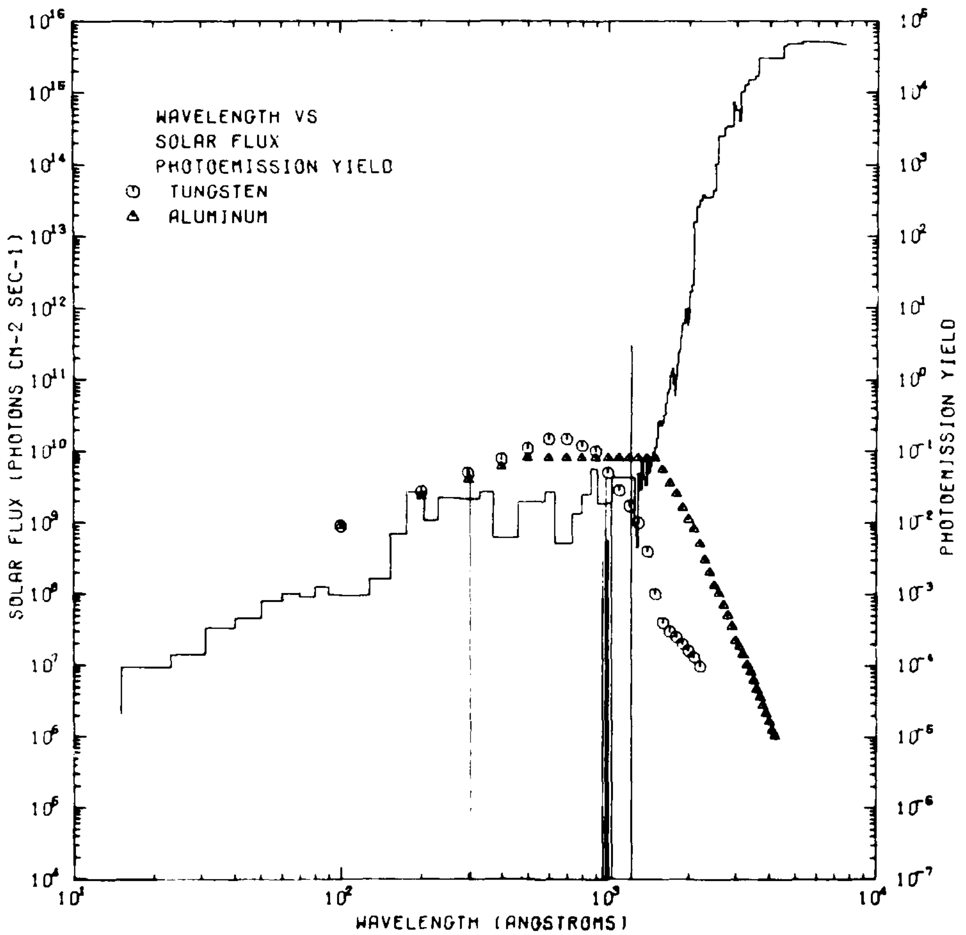

Figure 4. Solar Fluxes Corresponding to $F_{10.7}$ = 150, and Photoemission Yield of Aluminum and Tungsten, as a Function of Wavelength

Following Richmond,[4] the solar cycle variability of the fluxes has been parameterized in terms of the 10.7 cm radio flux as follows:

$$F_n = F_n^o(F'_{10.7}/F^o_{10.7,n})^{P_n} \tag{9}$$

where

$F'_{10.7} = F_{10.7} - 0.0573(F_{10.7} - 143.) - 0.001273(F_{10.7} - 143.)^2$

F_n = flux for the n^{th} band or line

F_n^o = flux at the solar activity level represented by $F^o_{10.7,n}$

P_n = a power derived from experimental data

The photoemission yields for aluminum and dirty tungsten, also shown in Figure 4, are representative of experimental and theoretical data presented by Whipple.[1] The long wavelength cutoff for dirty tungsten, which is dependent on the state of the metal surface, and which, according to Whipple,[1] varies between 1900 Å and 2600 Å, is taken here to be 2300 Å to best fit INJUN 5 observations (see Figure 7), as was empirically done by Garrett.[2]

The number densities of O, O_2, O_3, and N_2 below 100 km are from Strobel,[3] modified slightly within the 85 to 100 km height range to merge smoothly with the U.S. Standard Atmosphere (1976)[7] above 100 km. The NO profile is an average one, based on data in Swider.[8]

Note that considerations of wavelengths less than 700 Å and greater than 4500 Å, as well as absorption by N_2, NO, and H_2O, are not really germane to the computation of satellite photoelectron fluxes, but have nevertheless been included as options in the computer code for possible use in other environmental problems such as photoionization, atmospheric heating, and absorption by rocket effluents.

4. FORTRAN PROGRAM

The Appendix contains a listing of the FORTRAN program TESTL, sample input data, and sample output. TESTL is a main program written for the purpose of illustrating the use of the working subroutines ABSORB and INTEG. Subroutine ABSORB computes an array of wavelength-dependent percent atmospheric

---

7. U.S. Standard Atmosphere (1976), U.S. Government Printing Office, Washington, D.C.

8. Swider, W. (1972) E-region model parameters, J. Atmos. Terr. Phys. 34:1615-1626.

transmission coefficients $T(\lambda)$ for a given minimum ray path altitude (X_m). This involves interpolating the number densities of various absorbing species at altitudes along the ray path, finding the integrated densities of the species along the ray path (Eq. (6)), and multiplying by the wavelength-dependent absorption cross sections to compute the transmission coefficient (Eq. (5)). In conjunction with Subroutines FUNC and ANGIN, Subroutine INTEG performs the integration in Eq. (1). Given a wavelength in angstroms, Subroutine PYIELD gives the photoemission yields of aluminum and dirty tungsten by interpolating in tables.

Program TESTL illustrates the use of these subroutines to compute photoelectron fluxes for the INJUN 5 satellite. First, the wavelengths, solar flux values (ergs-cm^{-2}-sec^{-1}), the absorption cross sections (cm^2), and number densities (cm^{-3}) are read in from a data file (see Appendix for sample data files). An option is included to replace NO with H_2O as the fifth absorbing constituent. (This option has been utilized to examine the possible effects of water discharges from repeated launches of *Heavy Lift* Launch Vehicles (HLLV's) connected with proposed future Satellite Power System (SPS) activities.) The fluxes are then adjusted to the appropriate solar activity level, using Eq. (9), and converted from ergs-cm^{-2}-sec^{-1} to photons-cm^{-2}-sec^{-1}. The unattenuated photoelectron current is computed and printed out in amp-cm^{-2}. Finally, by calling ABSORB and INTEG, $P(X_m)$, the percentage of photoelectron flux as a function of X_m, is computed and printed out. Also printed are the transmission coefficients as a function of X_m and wavelength, and the quantity

$$PCURI = \frac{\int_{\lambda_1}^{\lambda} F_{\infty}(\lambda) P(\lambda)\, d\lambda}{\int_{\lambda_1}^{\infty} F_{\infty}(\lambda) P(\lambda)\, d\lambda} \tag{10}$$

which illustrates the relative contributions of various wavelengths to the photoelectron flux. See Appendix for a sample computer printout.

5. SAMPLE RESULTS

Some insight into the process of photoemission from a satellite surface can be obtained by examining results from the present model as a function of surface material, wavelength, and atmospheric absorbing species. In Figure 5, the percent of unattenuated photoelectron current, given by Eq. (10), is plotted as a

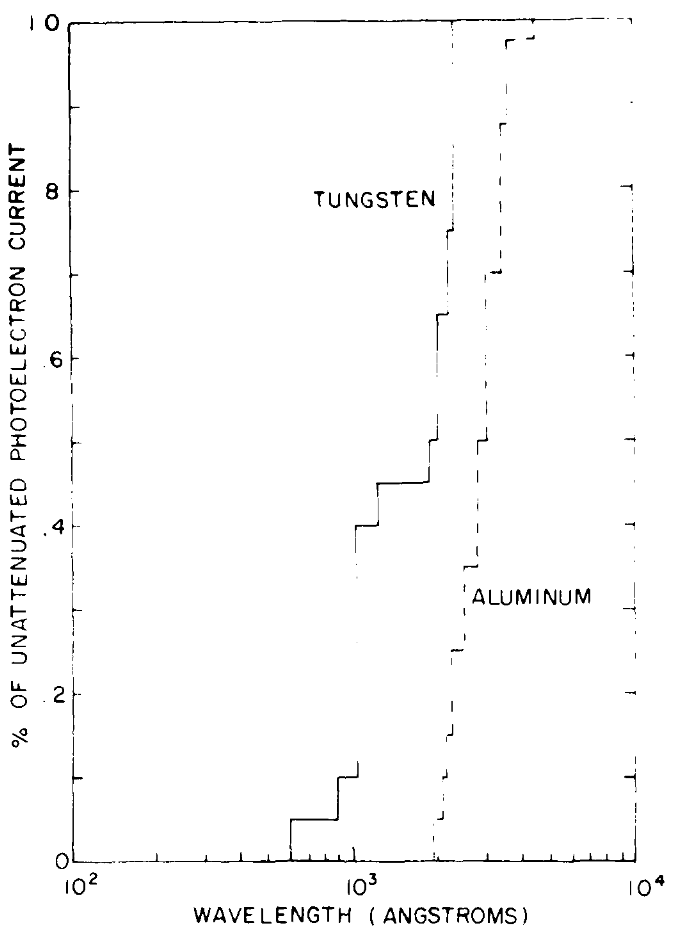

Figure 5. Percent of Unattenuated Photoelectron Current for Tungsten and Aluminum, Assuming Absorption by O, O_2, O_3, and N_2, and an $F_{10.7}$ Value of 150

function of wavelength for tungsten and aluminum, assuming $F_{10.7} = 150$. Here we see that 50 percent of the unattenuated photoelectron current is due to wavelengths less than 2000 Å for tungsten and 3000 Å for aluminum, and that 90 percent of the current can be attributed to wavelengths less than 2300 Å and 3600 Å, respectively, for tungsten and aluminum. The total unattenuated photoelectron currents corresponding to aluminum and tungsten are 0.293×10^{-6} amp-cm^{-2} and 0.167×10^{-8} amp-cm^{-2}, respectively, at solar minimum ($F_{10.7} = 50$), and 0.305×10^{-6} and 0.228×10^{-8} amp-cm^{-2} at solar maximum ($F_{10.7} = 250$). Thus, we see that photoemission from a tungsten surface, due to its greater dependence on shorter

wavelengths, is more variable with solar activity. Since most of the atmospheric absorption occurs below 150 km altitude, the solar cycle variation of thermospheric composition has been omitted in the present study.

The above differences in the wavelength dependence of photoemission rates for different materials suggest differences would exist with regard to the relative importance of absorbing species. For instance, from Input Table 1 in the Appendix we see that O, O_2, and O_3 are strong absorbers in the EUV, UV, and visible, respectively. Further, from the height dependences of these constituents, we would expect that EUV, UV, and visible radiations are absorbed at progressively lower heights in the atmosphere. These points are illustrated in Figure 6, where it is demonstrated that O_3 absorption of near-visible radiation can be neglected for tungsten photoemission in the case of EUV and aluminum. Note also that the 50 percent and 90 percent levels of unattenuated photoelectron current are attained above 55 km and 85 km, respectively, for aluminum, but above 95 km and 225 km, respectively, for tungsten.

In Figure 7, the percentage of photoelectron current measured by the INJUN 5 satellite shows good agreement with computations from the present model, assuming a tungsten surface and $F_{10.7}$ = 150. The only adjustment made to optimize this fit was to choose a long wavelength cutoff of 2300 A for the photoemission yield

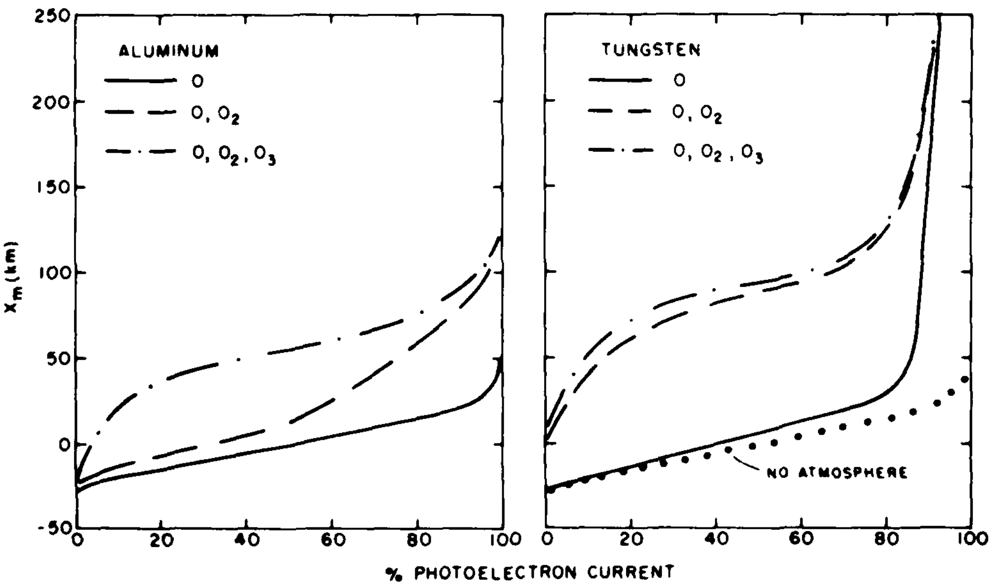

Figure 6. Percent of Photoelectron Current vs X_m for Aluminum and Tungsten for Different Combinations of Absorbing Species and an $F_{10.7}$ Value of 150

curve. According to an assessment of various experimental and theoretical data by Whipple,[1] this long wavelength cutoff, which is dependent on the state of the metal surface, varies between 1900 A and 2690 A for dirty tungsten.

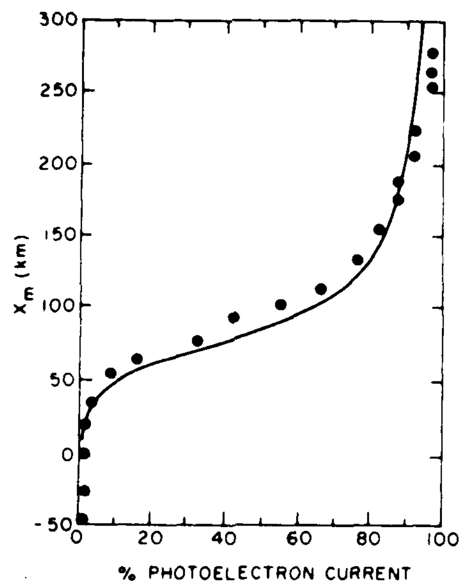

Figure 7. Theoretical Calculation of Percent of Photoelectron Current vs X_m for Tungsten and an $F_{10.7}$ Value of 150 Compared to INJUN 5 Observations

6. CONCLUSION

The model of atmospheric attenuation presented in this report, when coupled with models of the photoelectron emission characteristics of satellite material, provides an important step forward in our ability to study spacecraft charging. A number of increasingly more sophisticated models of the satellite charging process have been developed in the last year. One of those codes, the so-called NASCAP (NASA Spacecraft Charging Analyzer Program) model, is capable of modeling the complex surfaces and materials found on a typical satellite. Coupled with the knowledge of the solar flux as a function of satellite position, modeling of the penumbral passage of a satellite such as the AF/NASA P78-2 is possible—the simple model of Garrett[2] has already been used for this purpose. As the P78-2 instrumentation provides measurements of the potentials on several different types of

materials on the satellite, the model introduced here should prove extremely useful in allowing NASCAP to predict surface potentials during eclipse passage. It is to this end that the report has been prepared.

References

1. Whipple, E.C. (1965) The Equilibrium Potential of a Body in the Upper Atmosphere, NASA X-615-65-296.
2. Garrett, H.B. (1978) Effects of a Time-Varying Photoelectron Flux on Spacecraft Potential, AFGL-TR-78-0119, AD A058 993.
3. Strobel, D.F. (1976) Parameterization of the Atmospheric Heating Rate from 15 to 120 km Due to O_2 and O_3 Absorption of Solar Radiation, NRL Memorandum Report 3398.
4. Richmond, A.D. (1972) Numerical Model of the Equatorial Electrojet, AFCRL-72-0668, AD 758 196.
5. Keneshea, T.J. and Huffman, R.E. (1972) Solar Photoionization Rate Constants and Ultraviolet Intensities, AFCRL-72-0667, AD 756 480.
6. Banks, P.M. and Kockarts, G. (1973) Aeronomy, Part B, Academic Press, N.Y.
7. U.S. Standard Atmosphere (1976), U.S. Government Printing Office, Washington, D.C.
8. Swider, W. (1972) E-region model parameters, J. Atmos. Terr. Phys. 34:1615-1626.

PRECEDING PAGE BLANK-NOT FILMED

Appendix

Computer Program, Sample Input, and Sample Output

Main Program TESTL

```
      PROGRAM TESTL(INPUT,OUTPUT)
      COMMON/INFO1/Z1(150),Z2(150),FI(150),ABP(5,150),ILMAX,ILMIN,IN
      COMMON/INFO2/ZN(5,81),ZMAX,DZ,ZH(81),IZMAX
      DIMENSION T(150),P(10,150),NARRAY(6),XXM(9)
      DIMENSION I1(150),I2(150)
      DIMENSION BASE(150),POWER(150)
      DATA RS,XS,PE/.0043,1.4,1.0/
      DATA F107/150./
      DATA (BASE(I),I=1,136)/116*143.,5*177.,7*143.,8*150./
      DATA (POWER(I),I=1,136)/54*.0,1,45*.25,8*.5,4*.8,1.0,
     1     3*1.2,.8,9*1.2,3*1.7,2*2.3,2*2.6,3.0,3.5,5.0,6.7/
      DATA ZMAX,DZ/400.,5./
      DATA ILLA,LFIRST,LLAST,ILMAX/38,1,136,136/
      DATA IN/5/
      DATA INO,INH2O,PPMV/0,1,3./
      NARRAY(4)=1
      CALL SYSTEMC(115,NARRAY)
C
C        READ IN WAVELENGTH,SOLAR FLUX,ABSORPTION COEFF,AND
C        NUMBER DENSITIES OF ATMOSPHERIC CONSTITUENTS
C
  200 FORMAT(1X,I4,1X,I4,1X,1PE8.2,5(1PE8.1))
      DO 101 I=1,ILMAX
  101 READ 200,I1(I),I2(I),FI(I),(ABP(J,I),J=1,IN)
      IZMAX=(ZMAX/DZ+1.0001)
  300 FORMAT(1X,F4.0,5X,5(1PE8.2))
      DO 102 J=1,IZMAX
  102 READ 300,ZH(J),(ZN(I,J),I=1,IN)
 6001 FORMAT(////)
      PRINT 6000
      PRINT 6001
      DO 2010 I=1,45
 2010 PRINT 200,I1(I),I2(I),FI(I),(ABP(J,I),J=1,IN)
      PRINT 6000
      PRINT 6001
      DO 2011 I=46,90
 2011 PRINT 200,I1(I),I2(I),FI(I),(ABP(J,I),J=1,IN)
      PRINT 6000
      PRINT 6001
      DO 2012 I=91,136
 2012 PRINT 200,I1(I),I2(I),FI(I),(ABP(J,I),J=1,IN)
      PRINT 6000
      PRINT 6001
      DO 3010 I=1,40
 3010 PRINT 300, ZH(I),(ZN(J,I),J=1,IN)
      PRINT 6000
      PRINT 6001
      DO 3011 I=41,IZMAX
 3011 PRINT 300, ZH(I),(ZN(J,I),J=1,IN)
      PRINT 6000
C
C        IF INO=1 AND INH2O=0, NO IS FIFTH SPECIE
C        IF INO=0 AND INH2O=1, H2O IS FIFTH SPECIE
C        IF INH2O=1 DEFINE WATER CONC AND ABSORP COEFF HERE
      IF(INH2O.LT.1) GO TO 104
      ABP(5,ILLA)=1.4E-17
      PPV=PPMV*1.0E-06
      DO 103 J=1,IZMAX
      Z=(J-1)*5.
      IF(Z.LT.110.) ZN(5,J)=PPV*(ZN(1,J)+ZN(2,J)+ZN(4,J))
      IF(Z.GE.110.) ZN(5,J)=PPV*(ZN(1,23)+ZN(2,23)+ZN(4,23))
     1   *(ZN(1,J)/ZN(1,23))
  103 CONTINUE
  104 CONTINUE
C
C
C        ADJUST FLUX TO SOLAR ACTIVITY LEVEL,
C        CONVERT FLUX FROM ERG/CM2/SEC TO PHOTON/CM2/SEC,
C        AND COMPUTE UNATTENUATED PHOTOELECTRON FLUX (PCUR1).
C
      ILMIN=LFIRST
      ILMAX=LLAST
      XX=F107-143.
      F137=F107-XX*(.0537+.001273*XX)
      PCUR1=0.0
```

Main Program TESTL (Cont.)

```
      DO 3 I=ILMIN,ILMAX
      Z1(I)=I1(I)
      Z2(I)=I2(I)
      XLM=Z2(I)+(Z1(I)-Z2(I))/2.
      CALL PYIELD(XLM,PYA,PYT)
      FI(I)=FI(I)*F107/BASE(I)**POWER(I)
      FI(I)=FI(I)*XLM*.5E+08
    3 P(10,I)=PCURI=PCURI+FI(I)*PYT
      PCURI=PCURI/6.25E+18
 6000 FORMAT(1H1)
      PRINT 6000
 5000 FORMAT(1X,28HPCURI = INTEGRAL OF FI*PY = ,E15.3,2X,7HAMP/CM2)
      PRINT 5000, PCURI
      PCURI=PCURI*6.25E+18
C
C        COMPUTE PXM, PERCENTAGE OF PHOTOELECTRON FLUX
C        AS A FUNCTION OF XM
C
      DO 2 IXM=1,9
C        XM IS THE MINIMUM RAY PATH ALTITUDE
      XM=FLOAT(IXM-1)*50.
      ARGRC=((XM/6378.)+1.)/XS
      RC=ASIN(ARGRC)
C        RC IS THE ANGULAR DISTANCE IN RADIANS BETWEEN
C        CENTER OF EARTH AND SUN-SATELLITE LINE
      CALL ABSORB(XM,T)
      CALL INTEG(RC,FE,FS,XS,AILL)
      PXM(IXM)=AILL/PCURI
 4000 FORMAT(1X,3HXM=,F5.0,1X,4HPXM=,F10.3)
      PRINT 4000, XM, PXM(IXM)
      DO 1 I=ILMIN,ILMAX
    1 P(IXM,I)=T(I)
    2 CONTINUE
      DO 4 I=ILMIN,ILMAX
    4 P(10,I)=P(10,I)/PCURI
C
      PRINT 6000
 2001 FORMAT(30X,35H*********************    ATMOSPHERIC,1X,
     1 35HTRANSMISSION    *********************)
      PRINT 2001
 2000 FORMAT(12H WAVELENGTH ,7X,4HFLUX,8X,5HXM=0.0,2X,
     1    6HXM=50.,1X,7HXM=100.,1X,7HXM=150.,1X,7HXM=200.,
     2    1X,7HXM=250.,1X,7HXM=300.,1X,7HXM=350.,1X,7HXM=400.,
     3    4X,5HPCURI)
      PRINT 2000
 3000 FORMAT(1X,I4,1H-,I4,4X,E11.3,4X,9F8.5,2X,F8.5)
      PRINT 3000,(I1(I),I2(I),FI(I),(P(J,I),J=1,10),I=1,45)
      PRINT 6000
      PRINT 2001
      PRINT 2000
      PRINT 3000,(I1(I),I2(I),FI(I),(P(J,I),J=1,10),I=46,90)
      PRINT 6000
      PRINT 2001
      PRINT 2000
      PRINT 3000,(I1(I),I2(I),FI(I),(P(J,I),J=1,10),I=91,136)
      PRINT 6000
  202 FORMAT(12H WAVELENGTH ,3X,4HFLUX,12X,16H***O,O2,O3,N2,NO,1X,
     1 25HABSORPTION COEFFICIENTS***)
      PRINT 202
  201 FORMAT(1X,I4,1H-,I4,E11.3,4X,5F10.3)
      PRINT 201,   (I1(I),I2(I),FI(I),(ABP(J,I),J=1,IN),I=1,45)
      PRINT 6000
      PRINT 202
      PRINT 201,(I1(I),I2(I),FI(I),(ABP(J,I),J=1,IN),I=46,90)
      PRINT 6000
      PRINT 202
      PRINT 201,(I1(I),I2(I),FI(I),(ABP(J,I),J=1,IN),I=91,136)
      PRINT 6000
C     PRINT 300,   (ZM(I),(ZN(J,I),J=1,IN),I=1,IZMAX)
      STOP
      END
```

Subroutine ABSORB

```
      SUBROUTINE ABSORB(XM,T)
C        THIS SUBROUTINE COMPUTES AN ARRAY OF PERCENT ATMOSPHERIC
C        TRANSMISSION COEFFS (T) CORRESPONDING TO AN ARRAY OF
C        WAVELENGTH RANGES (Z1-Z2) FOR A GIVEN MINIMUM RAY PATH
C        ALTITUDE (XM). LENGTH OF ARRAYS = ILMAX-ILMIN.
C
      DIMENSION GAM(19),DELT(19),SUMN(5),T(150),XN(81),TN(5)
      DIMENSION S1(4),S2(4)
      COMMON/INFO1/Z1(150),Z2(150),FI(150),ABP(5,150),ILMAX,ILMIN,IN
      COMMON/INFO2/ZN(5,81),ZMAX,DZ,ZM(81),IZMAX
      DATA RE/6378./
C        TABLES OF COEFFS FOR SCHUMANN-RUNGE ABSORPTION BY O2
      DATA (GAM(I),I=1,19)/1.1363E-23,1.2652E-23,1.3033E-23,
     1  1.2899E-23,1.2204E-23,1.4514E-23,1.8859E-23,1.5313E-23,
     2  4.3235E-23,7.7757E-23,1.0341E-22,2.1377E-22,4.6929E-22,
     3  1.1067E-21,2.1219E-21,3.5317E-21,8.7466E-21,2.1935E-21,
     4  5.2693E-20/
      DATA (DELT(I),I=1,19)/6.4880E-14,9.6723E-14,3.6529E-13,
     1  1.7876E-12,2.6039E-12,5.493E-12,8.3986E-12,1.2232E-11,
     2  1.9898E-11,3.1147E-11,3.5539E-11,5.0541E-11,9.6615E-11,
     3  6.7463E-11,6.1449E-11,1.0362E-10,1.8609E-10,2.4514E-10,
     4  3.1771E-10/
C
      DO 3 I=ILMIN,ILMAX
    3 T(I)=1.0
      IF(XM.GE.ZMAX) GO TO 110
      A=SQRT((ZMAX+1.0E-10+RE)**2-(XM+RE)**2)
      DP=A/50.
      DO 2 I=1,IN
    2 SUMN(I)=0.0
C        INTERPOLATION OF CONSTITUENTS AT DETERMINED ALTITUDES.
      DO 1 I=1,50
      P=DP/2.+(I-1)*DP
      Z=SQRT((XM+RE)**2+P**2)-RE
      DO 1 N=1,IN
      DO 4 J=1,IZMAX
    4 XN(J)=ZN(N,J)
      CALL ATSM(Z,ZM,XN,IZMAX,1,S1,S2,3)
      CALL ALI(Z,S1,S2,XNZ,3,1.0E+12,IER)
      IF(N.EQ.3.AND.Z.GT.100.) XNZ=0.0
C        SUMMATION AND INTEGRATION OF NUMBER DENSITY WITH
C        ABSORPTION COEFFICIENT.
    1 SUMN(N)=SUMN(N)+XNZ
      FACTI=2.*DP*1.0E+05
      DO 5 N=1,IN
    5 TN(N)=SUMN(N)*FACTI
      IB=0
      DO 6 I=ILMIN,ILMAX
      SUMT=0.0
      DO 8 J=1,IN
      ILT=J-2
      IF(ILT) 113,112,113
  112 IF(I.GE.54.AND.I.LE.72) GO TO 111
  113 FABS=ABP(J,I)*TN(J)
      GO TO 8
  111 IB=IB+1
      FABS=GAM(IB)*TN(2)+DELT(IB)*SQRT(TN(2))
    8 SUMT=SUMT+FABS
  102 IF(SUMT.GT.10.) SUMT=10.
      T(I)=EXP(-SUMT)
    6 CONTINUE
  110 RETURN
      END
```

Subroutine PYIELD

```
      SUBROUTINE PYIELD(XA,PYA,PYT)
      DIMENSION PT(46),PA(46),A(46)
C
C         TABLE OF PHOTOEMISSION YIELDS - DIRTY TUNGSTEN
C
      DATA (PT(I),I=1,46)/.25E-03,.35E-02,.27E-01,.50E-01,
     1     .78E-01,.11E+00,.15E+00,.15E+00,.12E+00,.10E+00,
     2     .50E-01,.28E-01,.17E-01,.10E-01,.40E-02,.10E-02,
     3     .40E-03,.30E-03,.25E-03,.20E-03,.16E-03,.13E-03,
     4     .35E-04,23*(0.0)/
C
C         TABLE OF PHOTOEMISSION YIELDS - ALUMINUM
C
      DATA (PA(I),I=1,46)/46*(0.0)/
C
C         WAVELENGTH TABLE IN ANGSTROMS
C
      IF(XA.GE.4500.) PYA=PYT=0.0
      IF(XA.GE.4500.) GO TO 100
      DO 1 I=1,46
    1 A(I)=(I-1)*100.
C
C         INTERPOLATE LINEARLY
C
      IA=XA/100.+1.01
      FACT=(XA-A(IA))/100.
      PYA=(PA(IA+1)-PA(IA))*FACT+PA(IA)
      PYT=(PT(IA+1)-PT(IA))*FACT+PT(IA)
  100 RETURN
      END
```

Subroutine INTEG

```
      SUBROUTINE INTEG(RC,RE,RS,XS,AILL)
C
C        IN CONJUNCTION WITH SUBROUTINES FUNC AND ANGIN,
C        THIS SUBROUTINE INTEGRATES OVER THE UNOBSCURED PORTION
C        OF THE SOLAR DISK.
C
      DIMENSION RAD(21),Z(21)
      DR=RS/10.
      DO 1 I=1,11
      R=DR*(I-1)
      CALL ANGIN(R,RC,RE,XS,THE)
    1 RAD(I)=THE
      CALL QSF(DR,RAD,Z,11)
      AILL=Z(11)
      RSA=6.28318*(1.-COS(RS))
      AILL=AILL/RSA
      RETURN
      END
```

Subroutine FUNC

```
      SUBROUTINE FUNC(R,RC,RE,THT,F,XS)
      COMMON/INFO1/Z1(150),Z2(150),FI(150),ABP(5,150),ILMAX,ILMIN,IN
      DIMENSION T(150)
      AA=ACOS(COS(R)*COS(RC)+SIN(R)*SIN(RC)*COS(THT))
      XM=(XS*SIN(AA)-RE)*6378.
      FF=0.0
      IF(XM.LT.0.0) GO TO 2
      CALL ABSORB(XM,T)
      DO 1 I=ILMIN,ILMAX
      XLM=Z2(I)+(Z1(I)-Z2(I))/2.
      CALL PYIELD(XLM,PYA,PYT)
    1 FF=T(I)*FI(I)*PYT+FF
    2 F=FF*SIN(R)
      RETURN
      END
```

Subroutine ANGIN

```
      SUBROUTINE ANGIN(R,RC,FF,XS,THE)
      DIMENSION TH(21),Z(21)
      DTH=6.28318/10.
      DO 1 I=1,11
      THT=DTH*(I-1)
      CALL FUNC(R,RC,RE,THT,F,XS)
    1 TH(I)=F
      CALL QSF(DTH,TH,Z,11)
      THE=Z(11)
      RETURN
      END
```

Input Table 1. Solar Flux and σ as Functions of Wavelength

$\lambda_1 - \lambda_2$		$F_\infty(\lambda)$	σ O	σ O_2	σ O_3	σ N_2	σ NO
7550	7450	1.27E+04	0.	0.	3.5E-22	0.	0.
7450	7350	1.19E+04	0.	0.	3.8E-22	0.	0.
7350	7250	1.34E+04	0.	0.	4.2E-22	0.	0.
7250	7150	1.37E+04	0.	0.	5.4E-22	0.	0.
7150	7050	1.40E+04	0.	0.	6.5E-22	0.	0.
7050	6950	1.44E+04	0.	0.	8.2E-22	0.	0.
6950	6850	1.47E+04	0.	0.	1.0E-21	0.	0.
6850	6750	1.53E+04	0.	0.	1.3E-21	0.	0.
6750	6650	1.54E+04	0.	0.	1.6E-21	0.	0.
6650	6550	1.54E+04	0.	0.	2.0E-21	0.	0.
6550	6450	1.56E+04	0.	0.	2.4E-21	0.	0.
6450	6350	1.62E+04	0.	0.	2.9E-21	0.	0.
6350	6250	1.65E+04	0.	0.	3.4E-21	0.	0.
6250	6150	1.68E+04	0.	0.	3.9E-21	0.	0.
6150	6050	1.72E+04	0.	0.	4.5E-21	0.	0.
6050	5950	1.75E+04	0.	0.	4.6E-21	0.	0.
5950	5850	1.78E+04	0.	0.	4.9E-21	0.	0.
5850	5750	1.82E+04	0.	0.	4.3E-21	0.	0.
5750	5650	1.85E+04	0.	0.	4.3E-21	0.	0.
5650	5550	1.87E+04	0.	0.	3.5E-21	0.	0.
5550	5450	1.85E+04	0.	0.	3.1E-21	0.	0.
5450	5350	1.89E+04	0.	0.	2.7E-21	0.	0.
5350	5250	1.83E+04	0.	0.	2.3E-21	0.	0.
5250	5150	1.85E+04	0.	0.	1.7E-21	0.	0.
5150	5050	1.87E+04	0.	0.	1.5E-21	0.	0.
5050	4950	1.93E+04	0.	0.	9.4E-22	0.	0.
4950	4850	1.92E+04	0.	0.	6.7E-22	0.	0.
4850	4750	1.94E+04	0.	0.	5.7E-22	0.	0.
4750	4650	1.99E+04	0.	0.	2.7E-22	0.	0.
4650	4550	2.05E+04	0.	0.	2.4E-22	0.	0.
4550	4450	1.37E+04	0.	0.	1.2E-22	0.	0.
4450	3600	1.50E+05	0.	0.	2.0E-22	0.	0.
3600	3500	9.50E+03	0.	0.	3.5E-22	0.	0.
3500	3400	8.30E+03	0.	0.	1.0E-21	0.	0.
3400	3300	9.30E+03	0.	0.	4.2E-21	0.	0.
3300	3200	7.80E+03	0.	0.	1.5E-20	0.	0.
3200	3100	6.40E+03	0.	0.	6.2E-20	0.	0.
3100	3050	2.60E+03	0.	0.	1.5E-19	0.	0.
3050	2950	3.90E+03	0.	0.	3.5E-19	0.	0.
2950	2900	5.20E+03	0.	0.	1.2E-18	0.	0.
2900	2750	2.49E+03	0.	0.	3.3E-18	0.	0.
2750	2700	2.40E+03	0.	0.	5.8E-18	0.	0.
2700	2550	1.39E+03	0.	0.	1.0E-17	0.	0.
2550	2500	8.10E+02	0.	0.	1.1E-17	0.	0.
2500	2440	5.50E+02	0.	0.	9.8E-18	0.	0.
2440	2375	2.30E+02	0.	5.0E-25	8.2E-18	0.	0.
2375	2325	2.30E+02	0.	1.4E-24	6.4E-18	0.	0.
2325	2275	3.10E+02	0.	3.7E-24	4.5E-18	0.	0.
2275	2225	3.40E+02	0.	5.7E-24	3.0E-18	0.	0.
2225	2175	2.70E+02	1.	7.6E-24	1.8E-18	0.	0.
2175	2125	2.40E+02	1.	9.6E-24	1.0E-18	0.	0.
2125	2075	1.50E+02	0.	1.1E-23	5.5E-19	0.	0.
2075	2045	2.10E+01	0.	1.3E-23	3.8E-19	0.	0.
2045	2005	1.70E+01	0.	0.	3.3E-19	1.	0.
2005	1995	1.40E+01	0.	0.	3.1E-19	0.	0.
1995	1975	7.20E+00	0.	0.	3.3E-19	0.	0.
1975	1950	5.30E+00	0.	0.	3.6E-19	0.	0.
1950	1925	1.00E+01	0.	0.	4.1E-19	0.	0.
1925	1923	7.00E+00	0.	0.	4.5E-19	0.	0.
1923	1882	6.50E+00	0.	0.	5.2E-19	0.	0.
1882	1872	5.20E+00	0.	0.	5.9E-19	0.	0.
1872	1854	4.20E+00	0.	0.	6.5E-19	0.	0.
1854	1838	2.80E+00	0.	0.	6.8E-19	0.	0.
1838	1822	2.70E+00	0.	0.	7.0E-19	0.	0.
1822	1819	2.50E+00	0.	0.	7.3E-19	0.	0.
1819	1799	1.30E+00	0.	0.	7.5E-19	0.	0.
1799	1789	1.30E+00	0.	0.	7.7E-19	0.	0.
1789	1779	1.20E+00	1.	0.	7.9E-19	0.	0.

Input Table 1. Solar Flux and σ as Functions of Wavelength (Cont.)

$\lambda_1 - \lambda_2$		$F_\infty(\lambda)$	σ O	σ O_2	σ O_3	σ N_2	σ NO
1778	1772	9.10E-01	0.	0.	8.1E-19	0.	0.
1772	1766	6.70E-01	0.	0.	8.2E-19	0.	0.
1766	1760	1.37E+00	0.	0.	8.2E-19	0.	0.
1760	1749	1.08E+00	0.	0.	8.3E-19	0.	0.
1749	1730	1.70E+00	0.	3.7E-19	8.3E-19	0.	0.
1730	1710	1.59E+00	0.	5.9E-19	8.3E-19	0.	0.
1710	1690	1.30E+00	0.	9.5E-19	8.2E-19	0.	0.
1690	1670	9.70E-01	0.	1.7E-18	8.0E-19	0.	0.
1670	1650	7.70E-01	0.	1.8E-18	8.2E-19	0.	0.
1650	1630	5.60E-01	0.	2.9E-18	8.3E-19	0.	0.
1630	1610	4.90E-01	0.	3.4E-18	9.0E-19	0.	0.
1610	1590	3.20E-01	0.	4.7E-18	1.3E-19	0.	0.
1590	1570	2.90E-01	0.	6.0E-18	1.5E-18	0.	0.
1570	1550	3.40E-01	0.	7.3E-18	1.9E-18	0.	0.
1550	1530	3.30E-01	0.	9.5E-18	2.5E-18	0.	0.
1530	1510	2.00E-01	0.	1.0E-17	2.9E-18	0.	0.
1510	1490	1.50E-01	0.	1.1E-17	4.0E-18	0.	0.
1490	1470	1.30E-01	0.	1.2E-17	4.5E-18	0.	0.
1470	1450	1.10E-01	0.	1.3E-17	5.0E-18	0.	0.
1450	1430	8.30E-02	0.	1.5E-17	6.0E-18	0.	0.
1430	1410	7.00E-02	0.	1.5E-17	6.5E-18	0.	0.
1410	1390	1.30E-01	0.	1.4E-17	7.0E-18	0.	0.
1390	1370	4.80E-02	0.	1.3E-17	8.0E-18	0.	0.
1370	1350	6.30E-02	0.	9.0E-18	9.0E-18	0.	0.
1350	1330	1.20E-01	0.	2.3E-18	1.2E-17	0.	0.
1330	1310	4.30E-02	0.	1.4E-18	1.7E-17	0.	0.
1310	1290	7.60E-02	0.	5.0E-19	1.7E-17	0.	0.
1290	1270	6.90E-03	0.	2.8E-19	1.0E-17	0.	0.
1270	1250	1.60E-02	0.	4.3E-19	5.0E-18	0.	0.
1216	1215	5.00E+00	0.	1.0E-20	2.3E-17	0.	2.4E-18
1250	1027	7.60E-02	0.	2.0E-19	0.	1.0E-17	0.
1027	911	3.89E-02	0.	8.9E-18	0.	7.2E-19	0.
1026	1025	6.67E-02	0.	1.5E-18	0.	2.0E-21	0.
992	992	1.20E-02	0.	1.5E-18	0.	1.1E-19	0.
977	977	8.95E-02	0.	4.6E-18	0.	8.2E-20	0.
973	973	1.63E-02	0.	1.2E-17	0.	3.6E-16	0.
950	950	7.10E-03	0.	6.3E-18	0.	5.2E-18	0.
945	945	1.09E-03	0.	3.2E-18	0.	1.0E-19	0.
911	860	1.30E-01	3.0E-18	7.0E-18	0.	5.0E-18	0.
860	796	6.90E-02	2.8E-18	1.6E-17	0.	1.2E-17	0.
796	732	3.50E-02	3.0E-18	2.2E-17	0.	1.8E-17	0.
732	630	1.49E-02	7.5E-18	3.3E-17	0.	2.5E-17	0.
630	580	9.00E-02	9.5E-18	2.6E-17	0.	2.4E-17	0.
580	460	7.43E-02	9.8E-18	2.4E-17	0.	2.4E-17	0.
460	370	2.36E-02	9.6E-18	1.9E-17	0.	2.1E-17	0.
370	330	1.54E-01	9.7E-18	1.7E-17	0.	1.5E-17	0.
330	280	1.43E-01	8.2E-18	1.6E-17	0.	1.2E-17	0.
304	304	3.50E-01	8.2E-18	1.6E-17	0.	1.2E-17	0.
280	231	1.74E-01	7.5E-18	1.3E-17	0.	1.0E-17	0.
231	205	9.82E-02	5.5E-18	1.0E-17	0.	7.0E-18	0.
205	176	2.87E-01	4.0E-18	6.4E-18	0.	5.6E-18	0.
176	153	8.31E-02	3.8E-18	5.2E-18	0.	4.4E-18	0.
153	128	2.27E-02	2.1E-18	4.2E-18	0.	2.5E-18	0.
128	100	1.66E-02	1.4E-18	2.8E-18	0.	1.6E-18	0.
100	91	2.25E-02	1.1E-18	2.0E-18	0.	1.2E-18	0.
90	80	2.93E-02	7.6E-19	1.5E-18	0.	8.9E-19	0.
80	70	2.44E-02	5.6E-19	1.1E-18	0.	6.5E-19	0.
70	60	5.09E-02	3.6E-19	7.7E-19	0.	4.5E-19	0.
60	50	2.90E-02	2.5E-19	5.1E-19	0.	3.0E-19	0.
50	40	2.03E-02	1.5E-19	3.1E-19	0.	1.8E-19	0.
40	31	1.88E-02	8.2E-20	1.0E-19	0.	9.6E-20	0.
31	23	1.03E-02	4.5E-20	9.0E-20	0.	1.0E-19	0.
23	15	9.90E-03	3.5E-19	7.0E-19	0.	3.6E-19	0.
15	10	3.30E-03	1.4E-19	2.9E-19	0.	1.5E-19	0.
10	8	3.00E-04	5.6E-20	1.1E-19	0.	7.0E-20	0.
8	6	1.09E-04	3.2E-20	6.4E-20	0.	3.8E-20	0.
6	4	0.	1.5E-20	3.0E-20	0.	1.7E-20	0.
4	2	0.	4.3E-21	8.6E-21	0.	5.0E-21	0.

Input Table 2. Density (n) as a Function of Altitude X

X(km)	n(O)	n(O_2)	n(O_3)	n(N_2)	n(NO)
0.	3.70E+06	5.10E+18	8.00E+11	2.09E+19	0.
5.	3.00E+06	3.00E+18	7.00E+11	1.22E+19	0.
10.	3.00E+05	1.70E+18	9.00E+11	6.88E+18	0.
15.	3.00E+05	8.59E+17	1.80E+12	3.19E+18	0.
20.	1.00E+07	3.92E+17	3.10E+12	1.46E+18	0.
25.	5.00E+07	1.72E+17	4.50E+12	6.39E+17	0.
30.	2.00E+08	7.82E+16	3.10E+12	2.91E+17	0.
35.	3.50E+08	3.65E+16	1.60E+12	1.36E+17	0.
40.	1.50E+09	1.75E+16	6.70E+11	6.51E+16	0.
45.	3.00E+09	8.79E+15	2.10E+11	3.27E+16	0.
50.	9.00E+09	4.66E+15	7.00E+10	1.73E+16	0.
55.	2.00E+10	2.57E+15	2.20E+10	9.54E+15	0.
60.	2.50E+10	1.41E+15	7.00E+09	5.26E+15	1.15E+06
65.	2.30E+10	7.56E+14	2.20E+09	2.81E+15	1.73E+06
70.	2.00E+10	3.86E+14	7.00E+08	1.44E+15	3.00E+06
75.	4.00E+10	1.82E+14	2.00E+08	6.79E+14	5.00E+06
80.	4.20E+10	8.20E+13	3.10E+08	3.10E+14	8.00E+06
85.	1.70E+11	3.55E+13	1.20E+08	1.37E+14	2.00E+07
90.	2.44E+11	1.48E+13	2.70E+07	5.55E+13	3.00E+07
95.	4.37E+11	5.83E+12	4.63E+06	2.27E+13	3.70E+07
100.	4.30E+11	2.15E+12	1.30E+06	9.21E+12	3.85E+07
105.	3.91E+11	7.65E+11	1.50E+05	3.88E+12	4.00E+07
110.	2.35E+11	2.62E+11	1.40E+04	1.64E+12	3.30E+07
115.	1.43E+11	9.65E+10	1.20E+03	7.25E+11	3.50E+07
120.	9.28E+10	4.40E+10	1.50E+02	3.73E+11	3.00E+07
125.	6.38E+10	2.34E+10	0.	2.14E+11	2.30E+07
130.	4.63E+10	1.38E+10	0.	1.33E+11	1.75E+07
135.	3.50E+10	8.65E+09	0.	8.74E+10	1.32E+07
140.	2.73E+10	5.70E+09	0.	6.01E+10	1.00E+07
145.	2.18E+10	3.90E+09	0.	4.28E+10	8.00E+06
150.	1.78E+10	2.75E+09	0.	3.12E+10	6.00E+06
155.	1.48E+10	1.98E+09	0.	2.33E+10	4.30E+06
160.	1.24E+10	1.46E+09	0.	1.77E+10	4.00E+06
165.	1.05E+10	1.09E+09	0.	1.37E+10	3.30E+06
170.	9.00E+09	8.28E+08	0.	1.07E+10	2.25E+06
175.	7.77E+09	6.35E+08	0.	8.45E+09	1.90E+06
180.	6.75E+09	4.92E+08	0.	6.74E+09	1.30E+06
185.	5.90E+09	3.85E+08	0.	5.42E+09	1.00E+06
190.	5.18E+09	3.03E+08	0.	4.39E+09	0.
195.	4.57E+09	2.40E+08	0.	3.57E+09	0.
200.	4.05E+09	1.92E+08	0.	2.93E+09	0.
205.	3.61E+09	1.54E+08	0.	2.41E+09	0.
210.	3.21E+09	1.24E+08	0.	1.99E+09	0.
215.	2.87E+09	1.00E+08	0.	1.65E+09	0.
220.	2.57E+09	8.15E+07	0.	1.37E+09	0.
225.	2.31E+09	6.64E+07	0.	1.15E+09	0.
230.	2.08E+09	5.42E+07	0.	9.63E+08	0.
235.	1.88E+09	4.45E+07	0.	8.06E+08	0.
240.	1.70E+09	3.65E+07	0.	6.78E+08	0.
245.	1.53E+09	3.01E+07	0.	5.71E+08	0.
250.	1.39E+09	2.48E+07	0.	4.83E+08	0.
255.	1.26E+09	2.05E+07	0.	4.08E+08	0.
260.	1.14E+09	1.70E+07	0.	3.46E+08	0.
265.	1.04E+09	1.41E+07	0.	2.94E+08	0.
270.	9.45E+08	1.17E+07	0.	2.49E+08	0.
275.	8.60E+08	9.74E+06	0.	2.12E+08	0.
280.	7.83E+08	8.11E+06	0.	1.81E+08	0.
285.	7.14E+08	6.76E+06	0.	1.54E+08	0.
290.	6.52E+08	5.64E+06	0.	1.31E+08	0.
295.	5.95E+08	4.71E+06	0.	1.12E+08	0.
300.	5.43E+08	3.94E+06	0.	9.59E+07	0.
305.	5.06E+08	3.42E+06	0.	9.59E+07	0.
310.	4.54E+08	2.76E+06	0.	8.47E+07	0.
315.	4.23E+08	2.40E+06	0.	7.02E+07	0.
320.	3.80E+08	1.94E+06	0.	6.21E+07	0.
325.	3.54E+08	1.63E+06	0.	5.16E+07	0.
330.	3.13E+08	1.37E+06	0.	4.56E+07	0.
335.	2.97E+08	1.19E+06	0.	3.40E+07	0.
340.	2.68E+08	9.67E+05	0.	2.80E+07	0.
345.	2.50E+08	8.42E+05	0.	2.48E+07	0.
350.	2.25E+08	6.85E+05	0.	2.07E+07	0.
355.	2.10E+08	5.97E+05	0.	1.83E+07	0.
360.	1.89E+08	4.86E+05	0.	1.53E+07	0.
365.	1.78E+08	4.24E+05	0.	1.36E+07	0.
370.	1.53E+08	3.45E+05	0.	1.14E+07	0.
375.	1.49E+08	3.01E+05	0.	1.01E+07	0.
380.	1.34E+08	2.46E+05	0.	8.43E+06	0.
385.	1.26E+08	2.15E+05	0.	7.49E+06	0.
390.	1.14E+08	1.75E+05	0.	6.27E+06	0.
395.	1.06E+08	1.53E+05	0.	5.57E+06	0.
400.	9.58E+07	1.25E+05	0.	4.67E+06	0.

Output Table 1. Total Solar Flux in Wavelength Interval and Percent Transmission at Indicated Altitude (See Text)

		*********************			ATMOSPHERIC TRANSMISSION			*********************			
WAVELENGTH	FLUX	XM=0.0	XM=50.	XM=100.	XM=150.	XM=200.	XM=250.	XM=300.	XM=350.	XM=400.	PCUPI
7550-7450	.476E+16	.92143	.99893	1.00000	1.00000	1.00000	1.00000	1.00000	1.00000	1.00000	0.00000
7450-7350	.481E+16	.91499	.99890	1.00000	1.00000	1.00000	1.00000	1.00000	1.00000	1.00000	0.00000
7350-7250	.483E+16	.90648	.99879	1.00000	1.00000	1.00000	1.00000	1.00000	1.00000	1.00000	0.00000
7250-7150	.493E+16	.88140	.99844	1.00000	1.00000	1.00000	1.00000	1.00000	1.00000	1.00000	0.00000
7150-7050	.437E+16	.85902	.99812	1.00000	1.00000	1.00000	1.00000	1.00000	1.00000	1.00000	0.00000
7050-6950	.501E+16	.82555	.99763	1.00000	1.00000	1.00000	1.00000	1.00000	1.00000	1.00000	0.00000
6950-6850	.507E+16	.79153	.99711	1.00000	1.00000	1.00000	1.00000	1.00000	1.00000	1.00000	0.00000
6850-6750	.511E+16	.73792	.99625	1.00000	1.00000	1.00000	1.00000	1.00000	1.00000	1.00000	0.00000
6750-6650	.516E+16	.68794	.99538	1.00000	1.00000	1.00000	1.00000	1.00000	1.00000	1.00000	0.00000
6650-6550	.534E+16	.62653	.99423	1.00000	1.00000	1.00000	1.00000	1.00000	1.00000	1.00000	0.00000
6550-6450	.507E+16	.57059	.99308	1.00000	1.00000	1.00000	1.00000	1.00000	1.00000	1.00000	0.00000
6450-6350	.513E+16	.50765	.99165	1.00000	1.00000	1.00000	1.00000	1.00000	1.00000	1.00000	0.00000
6350-6250	.520E+16	.45164	.99022	1.00000	1.00000	1.00000	1.00000	1.00000	1.00000	1.00000	0.00000
6250-6150	.521E+16	.40162	.98879	1.00000	1.00000	1.00000	1.00000	1.00000	1.00000	1.00000	0.00000
6150-6050	.525E+16	.34921	.98707	1.00000	1.00000	1.00000	1.00000	1.00000	1.00000	1.00000	0.00000
6050-5950	.525E+16	.34116	.98673	1.00000	1.00000	1.00000	1.00000	1.00000	1.00000	1.00000	0.00000
5950-5850	.525E+16	.39253	.98850	1.00000	1.00000	1.00000	1.00000	1.00000	1.00000	1.00000	0.00000
5850-5750	.528E+16	.36595	.98764	1.00000	1.00000	1.00000	1.00000	1.00000	1.00000	1.00000	0.00000
5750-5650	.522E+16	.36595	.98764	1.00000	1.00000	1.00000	1.00000	1.00000	1.00000	1.00000	0.00000
5650-5550	.519E+16	.44121	.98933	1.00000	1.00000	1.00000	1.00000	1.00000	1.00000	1.00000	0.00000
5550-5450	.503E+16	.48446	.99108	1.00000	1.00000	1.00000	1.00000	1.00000	1.00000	1.00000	0.00000
5450-5350	.511E+16	.53135	.99222	1.00000	1.00000	1.00000	1.00000	1.00000	1.00000	1.00000	0.00000
5350-5250	.501E+16	.58409	.99337	1.00000	1.00000	1.00000	1.00000	1.00000	1.00000	1.00000	0.00000
5250-5150	.491E+16	.67204	.99513	1.00000	1.00000	1.00000	1.00000	1.00000	1.00000	1.00000	0.00000
5150-5050	.477E+16	.70421	.99567	1.00000	1.00000	1.00000	1.00000	1.00000	1.00000	1.00000	0.00000
5050-4950	.483E+16	.80271	.99729	1.00000	1.00000	1.00000	1.00000	1.00000	1.00000	1.00000	0.00000
4950-4850	.471E+16	.85502	.99806	1.00000	1.00000	1.00000	1.00000	1.00000	1.00000	1.00000	0.00000
4850-4750	.466E+16	.87524	.99835	1.00000	1.00000	1.00000	1.00000	1.00000	1.00000	1.00000	0.00000
4750-4650	.468E+16	.93883	.99922	1.00000	1.00000	1.00000	1.00000	1.00000	1.00000	1.00000	0.00000
4650-4550	.467E+16	.94544	.99931	1.00000	1.00000	1.00000	1.00000	1.00000	1.00000	1.00000	0.00000
4550-4450	.443E+16	.97234	.99965	1.00000	1.00000	1.00000	1.00000	1.00000	1.00000	1.00000	0.00000
4450-3600	.302E+16	.95432	.99942	1.00000	1.00000	1.00000	1.00000	1.00000	1.00000	1.00000	0.00000
3600-3500	.169E+16	.92143	.99899	1.00000	1.00000	1.00000	1.00000	1.00000	1.00000	1.00000	0.00000
3500-3400	.154E+16	.79153	.99711	1.00000	1.00000	1.00000	1.00000	1.00000	1.00000	1.00000	0.00000
3400-3300	.151E+16	.37460	.98793	1.00000	1.00000	1.00000	1.00000	1.00000	1.00000	1.00000	0.00000
3300-3200	.127E+16	.02995	.95755	1.00000	1.00000	1.00000	1.00000	1.00000	1.00000	1.00000	0.00000
3200-3100	.101E+16	.00005	.83567	1.00000	1.00000	1.00000	1.00000	1.00000	1.00000	1.00000	0.00000
3100-3050	.401E+15	.00005	.64808	1.00000	1.00000	1.00000	1.00000	1.00000	1.00000	1.00000	0.00000
3050-2950	.585E+15	.00005	.36347	1.00000	1.00000	1.00000	1.00000	1.00000	1.00000	1.00000	0.00000
2950-2900	.761E+15	.00005	.03112	1.00000	1.00000	1.00000	1.00000	1.00000	1.00000	1.00000	0.00000
2900-2750	.333E+15	.00005	.00007	1.00000	1.00000	1.00000	1.00000	1.00000	1.00000	1.00000	0.00000
2750-2700	.327E+15	.00005	.00005	1.00000	1.00000	1.00000	1.00000	1.00000	1.00000	1.00000	0.00000
2700-2550	.243E+15	.00005	.00005	1.00000	1.00000	1.00000	1.00000	1.00000	1.00000	1.00000	0.00000
2550-2500	.102E+15	.00005	.00005	1.00000	1.00000	1.00000	1.00000	1.00000	1.00000	1.00000	0.00000
2500-2440	.412E+14	.00005	.00005	1.00000	1.00000	1.00000	1.00000	1.00000	1.00000	1.00000	0.00000

Output Table 1. Total Solar Flux in Wavelength Interval and Percent Transmission at Indicated Altitude (See Text) (Cont.)

		**********************			ATMOSPHERIC	TRANSMISSION		**********************			
WAVELENGTH	FLUX	XM=0.0	XM=50.	XM=100.	XM=150.	XM=200.	XM=250.	XM=300.	XM=350.	XM=400.	FLUFT
2440-2375	.343E+14	.00005	.00005	.99995	1.00000	1.00000	1.00000	1.00000	1.00000	1.00000	0.00000
2375-2325	.341E+14	.00005	.00005	.99987	1.00000	1.00000	1.00000	1.00000	1.00000	1.00000	0.00000
2325-2275	.357E+14	.00005	.00005	.99959	1.00000	1.00000	1.00000	1.00000	1.00000	1.00000	0.00000
2275-2225	.383E+14	.00005	.00105	.99953	1.00000	1.00000	1.00000	1.00000	1.00000	1.00000	.08802
2225-2175	.313E+14	.00005	.00072	.99929	1.00000	1.00000	1.00000	1.00000	1.00000	1.00000	.23483
2175-2123	.259E+14	.00005	.00426	.99910	1.00000	1.00000	1.00000	1.00000	1.00000	1.00000	.37544
2125-2075	.159E+14	.00005	.01076	.99897	1.00000	1.00000	1.00000	1.00000	1.00000	1.00000	.47463
2075-2045	.206E+13	.00005	.01133	.99978	1.00000	1.00000	1.00000	1.00000	1.00000	1.00000	.48381
2045-2015	.172E+13	.00005	.01511	.99925	.99997	.99999	1.00000	1.00000	1.00000	1.00000	.50152
2015-1995	.142E+13	.00005	.01313	.99788	.99995	.99999	1.00000	1.00000	1.00000	1.00000	.51249
1995-1975	.793E+12	.00005	.01018	.99583	.99985	.99996	.99998	.99999	1.00000	1.00000	.51814
1975-1963	.579E+12	.00005	.00995	.99166	.99914	.99975	.99991	.99996	.99998	1.00000	.52239
1969-1925	.394E+12	.00005	.00292	.97325	.99871	.99967	.99986	.99994	.99998	1.00000	.53157
1925-1923	.681E+12	.00005	.00033	.94593	.99737	.99924	.99972	.99989	.99995	1.00000	.53785
1923-1882	.625E+12	.00005	.00005	.92030	.99598	.99884	.99957	.99983	.99993	1.00000	.54388
1882-1872	.494E+12	.00005	.00005	.88708	.99415	.99831	.99937	.99975	.99990	1.00000	.54893
1872-1854	.396E+12	.00005	.00005	.82102	.99050	.99725	.99898	.99959	.99983	1.00000	.55312
1854-1838	.261E+12	.00005	.00005	.73437	.98517	.99571	.99840	.99935	.99974	1.00000	.55599
1838-1822	.259E+12	.00005	.00005	.73208	.98309	.99510	.99818	.99926	.99970	1.00000	.55883
1822-1810	.239E+12	.00005	.00005	.60364	.97603	.99304	.99741	.99895	.99957	1.00000	.56152
1810-1798	.164E+12	.00005	.00005	.39313	.95741	.98755	.99536	.99811	.99923	1.00000	.56349
1798-1785	.119E+12	.00005	.00005	.45952	.96798	.99071	.99655	.99860	.99943	1.00000	.56494
1785-1773	.138E+12	.00005	.00005	.45229	.97052	.99151	.99685	.99872	.99948	1.00000	.56629
1778-1772	.727E+11	.00005	.00005	.27599	.95091	.98573	.99469	.99784	.99912	1.00000	.56722
1772-1766	.593E+11	.00005	.00005	.07277	.91287	.97446	.99048	.99613	.99842	1.00000	.56799
1766-1761	.116E+12	.00005	.00005	.01195	.88472	.96630	.98745	.99490	.99792	1.00000	.56950
1760-1740	.985E+11	.00005	.00005	.00033	.84848	.95610	.98370	.99338	.99730	1.00000	.57067
1740-1730	.149E+12	.00005	.00005	.00005	.91858	.99297	.99903	.99984	.99997	1.00000	.57271
1730-1719	.137E+12	.00005	.00005	.00005	.87334	.98881	.99845	.99974	.99996	1.00000	.57455
1719-1690	.112E+12	.00005	.00005	.00005	.82278	.98392	.99777	.99963	.99994	1.00000	.57617
1690-1670	.733E+11	.00005	.00005	.00005	.75924	.97737	.99685	.99948	.99991	1.00000	.57732
1670-1650	.546E+11	.00005	.00005	.00005	.66156	.96624	.99527	.99922	.99987	1.00000	.57838
1650-1630	.464E+11	.00005	.00005	.00005	.56336	.95343	.99344	.99892	.99982	1.00000	.57919
1630-1610	.329E+11	.00005	.00005	.00005	.45822	.93721	.99109	.99853	.99975	1.00000	.57979
1610-1590	.253E+11	.00005	.00005	.00005	.34001	.91424	.98771	.99796	.99966	1.00000	.58023
1590-1570	.232E+11	.00005	.00005	.00005	.29228	.89184	.98434	.99740	.99957	1.00000	.58089
1570-1550	.268E+11	.00005	.00005	.00005	.18721	.87001	.98197	.99684	.99947	1.00000	.58171
1550-1530	.257E+11	.00005	.00005	.00005	.14213	.85031	.97788	.99632	.99939	1.00000	.58265
1530-1510	.154E+11	.00005	.00005	.00005	.10073	.82612	.97403	.99567	.99928	1.00000	.58331
1510-1490	.114E+11	.00005	.00005	.00005	.08007	.81071	.97147	.99524	.99920	1.00000	.58386
1490-1470	.973E+10	.00005	.00005	.00005	.06365	.79539	.96892	.99481	.99913	1.00000	.58461
1470-1450	.912E+10	.00005	.00005	.00005	.05059	.78036	.96637	.99437	.99906	1.00000	.58549
1450-1430	.604E+10	.00005	.00005	.00005	.03197	.75114	.96130	.99351	.99892	1.00000	.58637
1430-1410	.503E+10	.00005	.00005	.00005	.03197	.75114	.96130	.99351	.99892	1.00000	.58712
1410-1390	.321E+10	.00005	.00005	.00005	.04022	.76561	.96383	.99394	.99899	1.00000	.58891

Output Table 1. Total Solar Flux in Wavelength Interval and Percent Transmission at Indicated Altitude (See Text) (Cont.)

WAVELENGTH	FLUX	XH=0.0	XH=50.	XH=100.	XH=150.	XH=200.	XH=250.	XH=300.	XH=350.	XH=400.	FLURI
		*********************			ATMOSPHERIC TRANSMISSION			*********************			
1390-1370	.135E+10	.00005	.00005	.00005	.05059	.78036	.96637	.99437	.99906	1.00000	.58975
1370-1350	.437E+10	.00005	.00005	.00005	.15941	.85846	.97917	.99653	.99942	1.00000	.59109
1350-1330	.913E+10	.00005	.00005	.00005	.58983	.95707	.99397	.99900	.99983	1.00000	.59499
1330-1310	.287E+11	.00005	.00005	.00005	.72517	.97365	.99632	.99939	.99990	1.00000	.59531
1310-1290	.500E+10	.00005	.00005	.00005	.89157	.99051	.99869	.99978	.99996	1.00000	.59773
1290-1270	.547E+09	.00005	.00005	.00005	.93775	.99467	.99926	.99988	.99998	1.00000	.59797
1270-1250	.102E+11	.00005	.00005	.00005	.90602	.99183	.99887	.99981	.99997	1.00000	.59861
1216-1215	.307E+12	.00005	.00005	.39216	.99690	.99959	.99985	.99996	.99999	1.00000	.83501
1250-1027	.438E+10	.00005	.00005	.00005	.00005	.54430	.57592	.88453	.97742	1.00000	.84104
1027- 911	.158E+11	.00005	.00005	.00005	.00005	.08989	.65700	.91232	.98307	1.00000	.84681
1026-1025	.359E+10	.00005	.00005	.00005	.70470	.97118	.99595	.99932	.99989	1.00000	.85352
992- 992	.603E+09	.00005	.00005	.00005	.53864	.94201	.99958	.99812	.99966	1.00000	.85511
977- 977	.447E+10	.00005	.00005	.00005	.31784	.90318	.98507	.99726	.99952	1.00000	.86542
973- 973	.911E+09	.00005	.00005	.00005	.00005	.00005	.00005	.01194	.43864	1.00000	.87092
950- 950	.345E+09	.00005	.00005	.00005	.00005	.17572	.73843	.91567	.98775	1.00000	.87217
945- 945	.318E+08	.00005	.00005	.00005	.02973	.68912	.93843	.99644	.99749	1.00000	.87252
911- 860	.589E+10	.00005	.00005	.00005	.00005	.03389	.40360	.73868	.90621	1.00000	.90185
860- 796	.257E+10	.00005	.00005	.00005	.00005	.00362	.27915	.65610	.89643	1.00000	.91611
796- 732	.139E+10	.00005	.00005	.00005	.00005	.00044	.18949	.62575	.87876	1.00000	.92489
732- 630	.526E+09	.00005	.00005	.00005	.00005	.00005	.04988	.39962	.75892	1.00000	.92871
630- 580	.282E+10	.00005	.00005	.00005	.00005	.00005	.03567	.34612	.71837	1.00000	.94920
580- 460	.202E+10	.00005	.00005	.00005	.00005	.00005	.03372	.33825	.71228	1.00000	.96075
460- 370	.648E+09	.00005	.00005	.00005	.00005	.00005	.04200	.35733	.72159	1.00000	.96335
370- 330	.284E+10	.00005	.00005	.00005	.00005	.00005	.07364	.41350	.75089	1.00000	.97216
330- 280	.230E+10	.00005	.00005	.00005	.00005	.00017	.09256	.44659	.76709	1.00000	.97789
304- 304	.551E+10	.00005	.00005	.00005	.00005	.00017	.09256	.44659	.76709	1.00000	.99154
280- 231	.182E+10	.00005	.00005	.00005	.00005	.00054	.12319	.49454	.78650	1.00000	.99504
231- 205	.874E+09	.00005	.00005	.00005	.00005	.00238	.17535	.54436	.81526	1.00000	.99636
205- 176	.223E+11	.00005	.00005	.00005	.00005	.01617	.31878	.67739	.87927	1.00000	.99909
176- 153	.558E+09	.00005	.00005	.00005	.00005	.04227	.41918	.74471	.90757	1.00000	.99965
153- 128	.130E+09	.00005	.00005	.00005	.00005	.12943	.56093	.81917	.93557	1.00000	.99975
128- 100	.393E+08	.00005	.00005	.00005	.00033	.26124	.68266	.87620	.95672	1.00000	.99981
100- 90	.103E+09	.00005	.00005	.00005	.00281	.37659	.75893	.91928	.96876	1.00000	.99985
90- 80	.131E+09	.00005	.00005	.00005	.01229	.47951	.81194	.93653	.97622	1.00000	.99990
80- 70	.966E+08	.00005	.00005	.00005	.04062	.58625	.85971	.94916	.98272	1.00000	.99993
70- 60	.109E+09	.00005	.00005	.00005	.11343	.69898	.90445	.95611	.98860	1.00000	.99996
60- 50	.861E+08	.00005	.00005	.00005	.22968	.78322	.93334	.97650	.99210	1.00000	.99998
50- 40	.493E+08	.00005	.00005	.00005	.41331	.86357	.95944	.98583	.99525	1.00000	.99999
40- 31	.331E+08	.00005	.00005	.00005	.62241	.92380	.97777	.99226	.99741	1.00000	1.00000
31- 23	.138E+08	.00005	.00005	.00005	.05527	.71289	.93748	.99425	.99642	1.00000	1.00000
23- 15	.333E+07	.00005	.00005	.00005	.15116	.72386	.91098	.95737	.98969	1.00000	1.00000
15- 10	.205E+07	.00005	.00005	.00005	.46082	.87694	.96305	.98699	.99561	1.00000	1.00000
10- 8	.134E+06	.00005	.00005	.00005	.71438	.94599	.98452	.99466	.99822	1.00000	1.00000
8- 6	.345E+05	.00005	.00005	.00005	.82953	.96935	.99123	.99697	.99899	1.00000	1.00000
6- 4	0.	.00005	.00005	.00315	.91820	.98576	.99593	.99859	.99953	1.00000	1.00000
4- 2	0.	.00005	.00005	.04179	.97549	.99586	.99382	.99959	.99986	1.00000	1.00000

Output Table 2. Absorption Coefficients as Functions of Wavelength

WAVELENGTH	FLUX	***C,O2,O3,N2,NO ABSORPTION COEFFICIENTS***				
7550-7450	.478E+15	0.	0.	.350E-21	0.	0.
7450-7350	.481E+16	0.	0.	.340E-21	0.	0.
7350-7250	.499E+15	0.	0.	.420E-21	0.	0.
7250-7150	.493E+16	0.	0.	.540E-21	0.	0.
7150-7050	.437E+16	0.	0.	.650E-21	0.	0.
7050-6950	.511E+16	0.	0.	.820E-21	0.	0.
6950-6850	.517E+16	0.	0.	.100E-20	0.	0.
6850-6750	.510E+16	0.	0.	.130E-20	0.	0.
6750-6650	.516E+16	0.	0.	.150E-20	0.	0.
6650-6550	.518E+16	0.	0.	.210E-20	0.	0.
6550-6450	.537E+16	0.	0.	.240E-20	0.	0.
6450-6350	.519E+16	0.	0.	.230E-20	0.	0.
6350-6250	.520E+16	0.	0.	.390E-20	0.	0.
6250-6150	.521E+16	0.	0.	.390E-20	0.	0.
6150-6050	.525E+16	0.	0.	.450E-20	0.	0.
6050-5950	.525E+16	0.	0.	.460E-20	0.	0.
5950-5850	.525E+16	0.	0.	.400E-20	0.	0.
5850-5750	.528E+16	0.	0.	.430E-20	0.	0.
5750-5650	.522E+16	0.	0.	.430E-20	0.	0.
5650-5550	.513E+16	0.	0.	.330E-20	0.	0.
5550-5450	.509E+16	0.	0.	.310E-20	0.	0.
5450-5350	.511E+16	0.	0.	.270E-21	0.	0.
5350-5250	.501E+16	0.	0.	.230E-20	0.	0.
5250-5150	.431E+16	0.	0.	.170E-20	0.	0.
5150-5050	.477E+16	0.	0.	.150E-20	0.	0.
5050-4950	.433E+16	0.	0.	.940E-21	0.	0.
4950-4850	.471E+16	0.	0.	.770E-21	0.	0.
4850-4750	.466E+16	0.	0.	.570E-21	0.	0.
4750-4650	.458E+16	0.	0.	.270E-21	0.	0.
4650-4550	.460E+16	0.	0.	.240E-21	0.	0.
4550-4450	.443E+16	0.	0.	.120E-21	0.	0.
4450-3600	.312E+16	0.	0.	.200E-21	0.	0.
3600-3500	.139E+16	0.	0.	.350E-21	0.	0.
3500-3400	.154E+16	0.	0.	.110E-20	0.	0.
3400-3300	.151E+16	0.	0.	.420E-20	0.	0.
3300-3200	.127E+16	0.	0.	.150E-19	0.	0.
3200-3100	.101E+16	0.	0.	.620E-19	0.	0.
3100-3050	.410E+15	0.	0.	.150E-18	0.	0.
3050-2950	.585E+15	0.	0.	.330E-18	0.	0.
2950-2900	.751E+15	0.	0.	.120E-17	0.	0.
2900-2750	.379E+15	0.	0.	.330E-17	0.	0.
2750-2700	.327E+15	0.	0.	.690E-17	0.	0.
2700-2550	.249E+15	0.	0.	.100E-16	0.	0.
2550-2500	.112E+15	0.	0.	.110E-16	0.	0.
2500-2440	.437E+14	0.	0.	.930E-17	0.	0.
2440-2375	.349E+14	0.	.500E-24	.820E-17	0.	0.
2375-2325	.341E+14	0.	.140E-23	.640E-17	0.	0.
2325-2275	.357E+14	0.	.330E-23	.450E-17	0.	0.
2275-2225	.393E+14	0.	.530E-23	.330E-17	0.	0.
2225-2175	.310E+14	0.	.760E-23	.190E-17	0.	0.
2175-2125	.258E+14	0.	.960E-23	.190E-17	0.	0.
2125-2075	.158E+14	0.	.110E-22	.550E-18	0.	0.
2075-2045	.206E+13	0.	.130E-22	.390E-18	0.	0.
2045-2005	.172E+13	0.	0.	.330E-18	0.	0.
2005-1935	.142E+13	0.	0.	.310E-18	0.	0.
1995-1975	.703E+12	0.	0.	.330E-18	0.	0.
1975-1969	.578E+12	0.	0.	.350E-18	0.	0.
1969-1925	.994E+12	0.	0.	.410E-18	0.	0.
1925-1923	.691E+12	0.	0.	.450E-18	0.	0.
1923-1882	.625E+12	0.	0.	.520E-18	0.	0.
1882-1872	.434E+12	0.	0.	.530E-18	0.	0.
1872-1854	.336E+12	0.	0.	.650E-18	0.	0.
1854-1839	.261E+12	0.	0.	.690E-18	0.	0.
1839-1822	.250E+12	0.	0.	.700E-18	0.	0.
1822-1810	.230E+12	0.	0.	.730E-18	0.	0.
1810-1798	.164E+12	0.	0.	.750E-18	0.	0.
1798-1788	.118E+12	0.	0.	.770E-18	0.	0.
1788-1778	.108E+12	0.	0.	.790E-18	0.	0.
1778-1772	.727E+11	0.	0.	.810E-18	0.	0.
1772-1766	.530E+11	0.	0.	.820E-18	0.	0.
1766-1760	.116E+12	0.	0.	.820E-18	0.	0.
1760-1740	.995E+11	0.	.	.830E-18	0.	0.
1740-1730	.149E+12	0.	.370E-19	.830E-18	0.	0.
1730-1710	.130E+12	0.	.590E-18	.830E-18	0.	0.
1710-1690	.112E+12	0.	.860E-18	.820E-18	0.	0.

Output Table 2. Absorption Coefficients as Functions of Wavelength (Cont.)

WAVELENGTH	FLUX	***O,O2,O3,N2,NO ABSORPTION COEFFICIENTS***				
1690-1670	.730E+11	0.	.122E-17	.800E-18	0.	0.
1670-1650	.646E+11	0.	.180E-17	.820E-18	0.	0.
1650-1630	.464E+11	0.	.250E-17	.930E-18	0.	0.
1630-1610	.320E+11	0.	.340E-17	.910E-18	0.	0.
1610-1590	.254E+11	0.	.470E-17	.130E-17	0.	0.
1590-1570	.232E+11	0.	.600E-17	.150E-17	0.	0.
1570-1550	.258E+11	0.	.730E-17	.130E-17	0.	0.
1550-1530	.257E+11	0.	.850E-17	.250E-17	0.	0.
1530-1510	.154E+11	0.	.100E-16	.230E-17	0.	0.
1510-1490	.114E+11	0.	.110E-16	.430E-17	0.	0.
1490-1470	.973E+10	0.	.120E-16	.450E-17	0.	0.
1470-1450	.812E+10	0.	.130E-16	.510E-17	0.	0.
1450-1430	.634E+10	0.	.150E-16	.610E-17	0.	0.
1430-1410	.503E+10	0.	.150E-16	.650E-17	0.	0.
1410-1390	.920E+10	0.	.140E-16	.770E-17	0.	0.
1390-1370	.336E+10	0.	.130E-16	.830E-17	0.	0.
1370-1350	.437E+10	0.	.810E-17	.900E-17	0.	0.
1350-1330	.813E+10	0.	.230E-17	.121E-16	0.	0.
1330-1310	.297E+10	0.	.140E-17	.171E-16	0.	0.
1310-1290	.590E+10	0.	.520E-19	.171E-16	0.	0.
1290-1270	.447E+09	0.	.280E-18	.170E-16	0.	0.
1270-1250	.132E+10	0.	.430E-18	.590E-17	0.	0.
1216-1216	.317E+12	0.	.100E-19	.230E-16	0.	.140E-15
1250-1027	.438E+10	0.	.200E-18	0.	.100E-16	0.
1027- 911	.198E+10	0.	.880E-17	0.	.720E-17	0.
1026-1025	.350E+10	0.	.150E-17	0.	.200E-20	0.
992- 992	.630E+09	0.	.150E-17	0.	.100E-18	0.
977- 977	.447E+10	0.	.900E-17	0.	.820E-19	0.
973- 973	.811E+09	0.	.320E-16	0.	.360E-15	0.
933- 953	.345E+03	0.	.630E-17	0.	.521E-17	0.
949- 949	.318E+09	0.	.320E-17	0.	.101E-17	0.
911- 863	.599E+10	.300E-17	.700E-17	0.	.600E-17	0.
863- 796	.257E+10	.290E-17	.160E-16	0.	.121E-16	0.
796- 732	.139E+10	.330E-17	.220E-16	0.	.180E-16	0.
732- 679	.526E+09	.750E-17	.330E-16	0.	.251E-16	0.
633- 587	.292E+10	.350E-17	.260E-16	0.	.240E-16	0.
580- 460	.202E+10	.380E-17	.240E-16	0.	.241E-16	0.
460- 370	.648E+09	.360E-17	.190E-16	0.	.219E-16	0.
370- 330	.286E+10	.370E-17	.170E-16	0.	.150E-16	0.
330- 293	.230E+10	.920E-17	.160E-16	0.	.120E-16	0.
304- 304	.551E+10	.820E-17	.160E-16	0.	.120E-16	0.
290- 231	.192E+10	.791E-17	.130E-16	0.	.101E-16	0.
231- 205	.874E+09	.650E-17	.100E-16	0.	.701E-17	0.
205- 176	.223E+10	.400E-17	.640E-17	0.	.560E-17	0.
176- 153	.558E+09	.301E-17	.520E-17	0.	.441E-17	0.
153- 129	.130E+10	.210E-17	.429E-17	0.	.250E-17	0.
129- 100	.939E+08	.140E-17	.280E-17	0.	.161E-17	0.
100- 98	.133E+09	.100E-17	.200E-17	0.	.121E-17	0.
90- 80	.131E+09	.760E-18	.150E-17	0.	.891E-18	0.
80- 71	.966E+08	.550E-18	.110E-17	0.	.651E-18	0.
70- 60	.139E+09	.360E-18	.770E-18	0.	.451E-18	0.
60- 51	.861E+09	.290E-18	.510E-18	0.	.301E-18	0.
50- 40	.433E+09	.151E-18	.310E-18	0.	.181E-18	0.
40- 31	.331E+09	.920E-19	.160E-18	0.	.961E-19	0.
31- 23	.138E+09	.450E-19	.990E-19	0.	.101E-17	0.
23- 13	.933E+07	.351E-18	.706E-18	0.	.361E-18	0.
15- 10	.295E+07	.140E-18	.290E-18	0.	.151E-18	0.
10- 9	.134E+06	.569E-19	.110E-18	0.	.771E-19	0.
8- 5	.346E+05	.326E-19	.644E-19	0.	.381E-19	0.
6- 4	0.	.150E-19	.300E-19	0.	.171E-19	0.
4- 2	0.	.430E-20	.860E-21	0.	.504E-20	0.

END

DATE
FILMED

1-81

DTIC